

# Novel NPY2R agonist BI 1820237 provides synergistic anti-obesity efficacy when combined with the GCGR/GLP-1R dual agonist survodutide



Robert Augustin<sup>1,\*</sup>, Anouk Oldenburger<sup>1,3,4</sup>, Tamara Baader-Pagler<sup>1</sup>, Tina Zimmermann<sup>1</sup>, Jens Borghardt<sup>1</sup>, Jacob Hecksher-Sørensen<sup>2</sup>, Angela Baljuls<sup>1</sup>, Wolfgang Reindl<sup>1</sup>, Bartłomiej Krawczyk<sup>1</sup>, Eric Martel<sup>1</sup>, Albert Brennauer<sup>1</sup>, Stefan Peters<sup>1</sup>, Achim Grube<sup>1</sup>, Lise Biehl Rudkjaer<sup>2</sup>, Peter Haebel<sup>1</sup>

## SUMMARY

**Objective:** Nutrient-stimulated gut hormone peptide YY3–36 (PYY3–36) selectively activates the neuropeptide Y2 receptor (NPY2R) and reduces energy intake in humans. We describe the discovery and pharmacology of the long-acting NPY2R agonist BI 1820237 and its potential bodyweight-lowering efficacy alone and in combination with the glucagon receptor (GCGR)/glucagon-like peptide-1 receptor (GLP-1R) dual agonist survodutide.

**Methods & Results:** BI 1820237 dose-dependently reduced food intake and gastric emptying in lean mice. Significant bodyweight reductions were not observed with BI 1820237 alone in diet-induced obese mice, however combination with survodutide led to bodyweight reduction of 22% which was significantly ( $p < 0.01$ ) greater than the 17% bodyweight reduction with survodutide alone. Regression-based interaction analysis demonstrated that BI 1820237 increased the efficacy of survodutide by 265% at an ED50 of 11.7 nmol/kg over a range of dose combinations.

**Conclusion:** Synergistic NPY2R and GCGR/GLP-1R agonism provides an attractive mode of action for clinically relevant weight loss in patients with obesity.

© 2025 The Author(s). Published by Elsevier GmbH. This is an open access article under the CC BY-NC-ND license (<http://creativecommons.org/licenses/by-nc-nd/4.0/>).

**Keywords** PYY3–36; NPY; NPY2R; BI 1820237; Survodutide; Obesity; G protein coupled receptor

## 1. INTRODUCTION

Obesity has become a global epidemic with a prevalence of approximately 40% in the adult population in the US [1] and 25% in Europe [2]. It is associated with a decrease in life expectancy [3] and the emergence of comorbidities, such as type 2 diabetes (T2D), cardiovascular disease (CVD), metabolic dysfunction-associated steatohepatitis (MASH), certain cancers, Alzheimer's disease, and osteoarthritis, imposing a burden on healthcare systems [3–7]. With the recognition of obesity as a chronic, relapsing, progressive condition [8], and CVD and T2D representing two of the main causes of death in Western societies [9], efficacious therapeutic interventions are urgently needed. In recent years, research has successfully demonstrated that long-acting peptide mimetics are well-tolerated and provide efficacious pharmacological interventions that overcome the historical failures of obesity pharmacotherapies by leveraging a pharmacology-based approach mimicking entero-endocrine (e.g., glucagon-like peptide-1 (GLP-1), PYY3–36) and endo-pancreatic (e.g. amylin, glucagon) nutrient-stimulated peptide hormones [10]. GLP-1 and PYY3–36 are co-secreted from enteroendocrine L-cells of the distal ileum upon food

intake and both peptide hormones are known to promote satiety and delay gastric emptying, facilitating nutrient transit throughout the gastrointestinal tract. Named PYY because of a central tyrosine–tyrosine motif in its 36-amino acids structure, PYY1–36 and PYY3–36 are the two main endogenous forms of the peptide hormone, with the dipeptidyl peptidase-4 (DPP4) mediating the conversion of PYY1–36 to PYY3–36 [11]. PYY hormones mediate their effects via the five different Y-receptors (NPY1R, NPY2R, NPY4R, NPY5R, and NPY6R). These receptors differ in their tissue distribution, controlling various physiologies that include food intake and energy homeostasis [12,13]. While PYY1–36 binds to all Y-receptor subtypes, PYY3–36 selectively activates the NPY2R [14]. The human NPY2R shares a high (>90%) similarity across species. It signals via the G-protein  $G\alpha_i$ , whereby receptor activation leads to a decrease of cellular cyclic AMP [14]. The NPY2R is expressed throughout the central nervous system, particularly in the hypothalamus and the area postrema, sites of action that have been implicated in food intake reduction and emesis, respectively, caused by peripherally injected PYY3–36 or NPY2R agonists. The presence of the receptor in the nodose ganglion and vagal afferents has raised the possibility that PYY3–36 exerts its feeding

<sup>1</sup>Boehringer Ingelheim Pharma GmbH & Co. KG, Birkendorfer Str. 65, 88397, Biberach an der Riß, Germany <sup>2</sup>Gubra A/S, Hørsholm Kongevej 11B, 2970, Hørsholm, Denmark

<sup>3</sup> Robert Augustin and Anouk Oldenburger contributed equally to this work.

<sup>4</sup> Anouk Oldenburger was an employee of Boehringer Ingelheim at the time of the analysis but is now employed by Novo Nordisk.

\*Corresponding author. Boehringer Ingelheim International GmbH, Birkendorfer Str. 65, 88397, Biberach an der Riß, Germany. E-mail: [robert.augustin@boehringer-ingelheim.com](mailto:robert.augustin@boehringer-ingelheim.com) (R. Augustin).

Received April 11, 2025 • Revision received June 27, 2025 • Accepted July 1, 2025 • Available online 5 July 2025

<https://doi.org/10.1016/j.molmet.2025.102205>

effects by acting centrally, via vagal activation, or combinations of both [15]. In preclinical and clinical studies, peripheral administration of PYY3–36 has been demonstrated to suppress food intake and reduce bodyweight. The anorectic effects of NPY2R agonism have been suggested to involve central as well as peripheral mechanisms such as activation of neuronal centers in the forebrain and hindbrain regions (e.g., area postrema [AP], nucleus tractus solitarius [NTS]) [16] and inhibition of gastric emptying [17] acting on vagal afferents [18]. In both rodents and humans, co-administration of native PYY3–36 and GLP-1 or analogs thereof demonstrated a synergistic decrease in energy intake [19–22]. Beyond its effects on food intake, evidence that PYY3–36 improves glycemic control, insulin resistance, and lipid metabolism in rodents might suggest a potential therapeutic benefit in patients with obesity [23,24]. Potential dose-limiting gastrointestinal side effects observed with PYY3–36 administration in humans might be overcome by long-acting analogs, as recently suggested [20]. Clinically, well-tolerated and sustainable bodyweight-lowering efficacy for people with obesity might be achieved by combining the synergistic anorectic principle of GLP-1 and PYY3–36 with an energy expenditure increasing mechanism such as glucagon receptor (GCGR) agonism [25]. The GCGR/GLP-1 receptor (GLP-1R) dual agonist survodutide is currently investigated in phase III clinical studies in people living with obesity (SYNCHRONIZE™ trials) and in those living with MASH (LIVERAGE™ trials). Combination of survodutide with a long-acting NPY2R agonist may potentially provide additional bodyweight-lowering efficacy, with a favorable tolerability through the synergy of GLP-1R and NPY2R agonism further reducing caloric intake, compared with GLP-1R agonism alone. In addition, the GCGR agonism of survodutide is expected to increase metabolic rate (energy expenditure), thereby providing additional, sustainable weight lowering efficacy and loss of excess adipose tissue, mechanistically addressing an important aspect of energy homeostasis [26]. Here we describe the discovery and chemical nature of the long-acting NPY2R agonist BI 1820237 and its pharmacological characterization when combined with the GCGR/GLP-1R dual agonist survodutide.

## 2. MATERIAL AND METHODS

### 2.1. Peptide synthesis

Peptides were synthesized by microwave-assisted solid-phase peptide synthesis (SPPS) using a Fmoc strategy in dimethylformamide (DMF) on a polystyrene resin (TentaGel™ S RAM; Rapp Polymere GmbH, Tübingen, Germany). *N,N*-Diisopropylcarbodiimide (DIC) was used as coupling reagent together with ethyl-2-cyano-2-(hydroxyimino)acetate (Oxyma) as additive. Piperidine (10% in DMF) was used for deprotection. The crude peptide was cleaved from resin using 95/2.5/2.5% (v/v) TFA/TIS/water at 40 °C for 45 min, precipitated, purified by high-performance liquid chromatography–mass spectrometry, and lyophilized.

### 2.2. Functional potency and affinity for human NPY2R

The functional potency of BI 1820237 was determined in HEK293 cAMP response element (CRE)-luc2P cells (Promega) recombinantly expressing human NPY2R. The agonistic activity of BI 1820237 was assessed by measuring the inhibition of forskolin-induced cAMP generation in a homogeneous time-resolved fluorescence (HTRF) assay, as well as the reduction of CRE-dependent luciferase (CRE-Luc) activity. All tested peptides were produced in house, handled as 1 mM stock solution in dimethyl sulfoxide (DMSO), and tested within a final concentration range between 3.2 pM and 100 nM. Peptides were transferred into assay plates using acoustic dispensing with an ECHO

555 (Labcyte). Sound waves were used to transfer droplets of 2.5 nL from a source plate to a target plate with final sample concentrations and volumes achieved by combining the respective number of droplets of sample stocks and DMSO. Cells were cultured in Dulbecco's Modified Eagle Medium (with high glucose/L-glutamine) supplemented with 10% fetal bovine serum, 50 µg/mL hygromycin, and 400 µg/mL geneticin, and harvested at a confluency of 60–70%. For the cAMP HTRF assay, 5000 cells in 20 µL assay buffer (Krebs–Ringer Bicarbonate 4-(2-Hydroxyethyl)piperazine-1-ethane-sulfonic acid [HEPES] (KRBH) with 0.5 mM 3-isobutyl-1-methylxanthine [IBMX] and 0.5% human plasma) were added to each well containing spotted peptide and 5 µL of forskolin in assay buffer (final concentration 2 µM), and subsequently kept at 37 °C for 40 min in a humidified incubator. Afterwards, 5 µL of cAMP-Eu and 5 µL anti-cAMP-d2 (both as 1:50 pre-dilution in cAMP Gi Kit lysis buffer; Cisbio) were added and incubated for 1 h at room temperature (RT), followed by measuring the fluorescence resonance energy transfer signal in an EnVision™ 2104 multimode microplate reader (PerkinElmer, now Revvity). For the CRE-Luc assay, 30,000 cells in either 20 µL assay buffer (KRBH with 0.5 mM IBMX and 0.5% human plasma) or in 100% human plasma were added to each well containing spotted peptide and 5 µL of forskolin in assay buffer with 0.5% human plasma (final concentration 2 µM) or in 100% human plasma (final concentration 8 µM), followed by incubation for 4 h at 37 °C in a humidified incubator. Afterwards, plates were equilibrated to RT and 25 µL of Bright-Glo luciferase reagent (Promega) were added per well, incubated for 15 min at RT and the luminescence signal was measured on an EnVision™ 2104 multimode micro plate reader. The affinities of BI 1820237 for the human NPY1R, NPY2R, NPY4, and NPY5R were investigated by competitive binding assays using membrane preparations from cells recombinantly expressing each receptor. For the human NPY2R, membrane preparations were obtained from Chemiscreen™ (Chemicon®, HTS066M; Lot: SC20190226). For the human NPY1, 4, and 5 receptors, CHO–K1 cells stably expressing the respective receptors, were cultured in 1720 cm<sup>2</sup> hyperflasks with Ham's F12 medium (+10% FCS +400 µg/mL Geneticin) at 5% CO<sub>2</sub> and 37 °C. At 90% confluence, the cells were washed with 20 mL 37 °C pre-warmed Dulbecco's phosphate buffered saline (DPBS), 100 mL DPBS with 0.2% ethylenediaminetetraacetic acid (EDTA) was added, and the dishes were kept for 5 min at 5% CO<sub>2</sub> and 37 °C. The cells were tapped from the plate, rinsed with 50 mL DPBS with 0.2% EDTA, and pelleted by centrifugation in a 50 mL Falcon tube for 10 min, 210 *g* at 4 °C. The supernatant was removed, and the pellet was resuspended in 15 mL ice cold membrane isolation buffer (50 mM HEPES; 5 mM MgCl<sub>2</sub> \* 6H<sub>2</sub>O; 1 mM CaCl<sub>2</sub> \* 2H<sub>2</sub>O pH7.4; 0.32 mM sucrose; 5 mM Pefabloc SC). The cell suspension was homogenized with an ultrasonic processor twice for 45 s on ice, centrifuged for 1 min, 18 *g* at 4 °C, and the supernatant collected and centrifuged for 20 min, 48,000 *g* at 4 °C. The supernatant was removed, and the membrane pellet was resuspended in 25 mL ice cold membrane isolation buffer followed by a further homogenization as described earlier. Finally, the supernatant was removed, and the membranes were aliquoted in low protein binding tubes. The protein concentration of the membrane preparation was determined using Pierce™ bicinchoninic acid assay (Thermo Fisher Scientific) following the manufacturer's protocol. The membrane suspensions were stored at –80 °C until use. The dissociation constants (*K<sub>d</sub>*) for the different radioligands (for <sup>125</sup>I-PYY1–36 for NPY receptors 1, 2, and 5; <sup>125</sup>I-PP for NPY4R) were determined upon incubation of the respective membrane preparations with 1 nM of the <sup>125</sup>I-labeled tracer in a total volume of 100 µL in polypropylene-96-well-plates. Non-specific binding was measured by adding 1 µM of

either PYY3–36, or PP in case of the NPY4R. After incubation for 120 min at RT under shaking (450 rpm/min), the assay-mixture was harvested through glass fiber C grade (GF/C) filter plates, using a FilterMate™ Universal Harvester (PerkinElmer). Non-specific binding was reduced by incubating the GF/C plates with 0.5% PEI at RT overnight. The GF/C plates were washed 4 times with ice cold wash-buffer, dried for 2 h, and after sealing the bottom, 50  $\mu$ L/well Micro-Scint™-20 (Revvity) was added, and the plates were sealed with a TopSeal-A PLUS adhesive microplate seal (Revvity). After incubation in the dark for at least 30 min at RT, the counts per minute were measured with a TopCount liquid scintillation counter (Revvity). For BI 1820237, the half-maximal inhibitory concentration ( $IC_{50}$ ) was determined upon dilution of BI 1820237 in DMSO (100-fold final concentration) to final concentrations ranging from 0.01 nM to 1  $\mu$ M. Reagents were pipetted in the following order: 10  $\mu$ L assay buffer or compound-dilution, 10  $\mu$ L  $^{125}$ I-labeled ligand (final concentration 0.05 nM) and 80  $\mu$ L membranes (final concentration 5  $\mu$ g/well). The plates were incubated for 2 h at RT under shaking (450 rpm/min) and processed as described for the  $K_d$  determinations. Calculation of the affinity constant  $K_i$  was performed according to the Cheng–Prusoff equation  $K_i = IC_{50}/(1 + [S])/K_m$  [27]. The affinity of BI 1820237 for mouse and human NPY2R was determined by Epics Therapeutics (SA 47 rue Adrienne Bolland, 6041 Gosselies, Belgium) applying competitive radioligand binding assays using  $^{125}$ I-PYY as reporter ligand and compared with neuropeptide Y. Doseresponse curves were generated for  $EC_{50}$  and  $E_{max}$  determined using a four-parameter logistic fit model.

### 2.3. Pharmacokinetic studies

For pharmacokinetic analysis, male Naval Medical Research Institute (NMRI) mice (Charles River, Germany) were given a single intravenous or subcutaneous BI 1820237 dose (30 nmol/kg;  $N = 2$  for intravenous and  $N = 3$  for subcutaneous route). In addition, male beagle dogs (Boehringer Ingelheim/BASF, Germany) received an intravenous or subcutaneous dose of 1.25 nmol/kg ( $N = 2$ ) or 5 nmol/kg ( $N = 3$ ) BI 1820237, respectively. Plasma samples were generated at different time points post-dosing and stored at  $-20$  °C until further analysis. Plasma concentrations of BI 1820237 were measured using liquid chromatography/tandem mass spectrometry on a QTRAP 6500+ (Sciex, Framingham, MA, USA).

### 2.4. Acute food intake

Male NMRI mice were obtained from Charles River (Charles River, Research Models & Services Germany GmbH) or from Janvier (Janvier Labs, France) at 5 weeks of age. The animals were group-housed with 4 mice per cage under a 12/12 h dark–light cycle, light off at 3 PM. RT was controlled to  $21$  °C  $\pm$  1 °C, with  $60\% \pm 20\%$  humidity. Animals had ad libitum access to regular rodent chow (KLIBA Nafag 3430 or Altromin 1324, Brogaarden, Denmark) and tap water. Animals were transferred 5–7 days before the start of the study to a real-time food intake monitoring system (HM-2; MBRose, Denmark), to allow acclimatization to experimental conditions. As the animals were uniquely labeled with microchips, each individual animal was identified by its microchip upon entry and exit from the food channel. Randomization of mice for each study group ( $n = 7$ – $8$ ) was based on bodyweight measured the day before the start of the study. A vehicle-treated group was included in each experiment. Six hours before the start of the night phase, animals were fasted. One hour before the dark phase, animals

were dosed once subcutaneously with the compound. Food intake was reported hourly for a period of 24 h. The food intake of the treated groups was normalized (in %) to the average food intake of the group receiving vehicle.  $ED_{50}$  values were calculated in Prism 9 (GraphPad Software) using the nonlinear fit tool.

### 2.5. Acute gastric emptying in lean mice

Male C57BL/6JRj mice were obtained from Janvier (Janvier Labs, France) at 9–10 weeks of age. The animals were group-housed with 4 mice per cage under a 12/12 h dark–light cycle, light off at 6 PM. RT was controlled to  $21$  °C  $\pm$  1 °C, with  $60\% \pm 20\%$  humidity. Animals had ad libitum access to regular rodent chow (KLIBA Nafag 3430 or Altromin 1324, Brogaarden, Denmark) and tap water. To assess gastric emptying, animals were fasted for 8.5 h and a basal blood sample for glucose measurement was obtained in the morning for randomization. After another 30 min fasting, the compound was administered once subcutaneously. Three hours later, a glucose (2 g/kg) – acetaminophen (100 mg/kg) bolus was given by oral gavage (10 mL/kg). For acetaminophen and glucose measurements, blood samples were taken before the glucose load (20 min) and 10 min, 30 min, and 60 min thereafter. The animals received food again after the test and had ad libitum access to water throughout the study.

### 2.6. Subchronic, repeated dose study in diet-induced obese mice

Male C57BL6/J mice (Janvier Labs, France) were pre-fed on 60% high-fat diet (Research Diets, Inc., USA) starting at 6 weeks of age. Mice were single-housed to obtain accurate and individual food intake measurements of each animal and assigned a number. Animals were housed at a RT of  $21 \pm 2$  °C, relative humidity  $60\% \pm 20\%$  and a reversed 12-h light/dark cycle (light off at 10 AM). During the entire study, animals had ad libitum access to food and water. Before start of treatment, a stratified randomization was performed based on bodyweight at Week  $-1$ . At study start, the age of mice was 25 weeks. Before the start of compound treatments, groups were randomized based on bodyweight, with an average of 45 g. Bodyweight and food intake were measured before compound administration. Animals were dosed daily by subcutaneous injection around 1 h before start of the night phase. Control animals were dosed daily with vehicle, and were randomized according to their bodyweight before the start of treatment.

### 2.7. Light-sheet fluorescent microscopy

All samples were imaged using a Lavisision light-sheet ultramicroscope II (Miltényi Biotec GmbH, Bergisch Gladbach, Germany) with a Zyla 4.2PCL10 sCMOS camera (Andor Technology, Belfast, UK), a SuperK EXTREME supercontinuum white-light laser EXR-15 (NKT Photonics, Birkerød, Denmark) and an MV PLAPO 2  $\times$  C (Olympus, Tokyo, Japan) objective lens. Samples were mounted to a silicone sample holder (with ventral side up) and imaged in an ethyl cinnamate filled chamber. ImSpector microscope controller software (v7) was used (Miltényi Biotec GmbH, Bergisch Gladbach, Germany). Images were acquired at  $1.26\times$  total magnification using dual-sided illumination and 9 horizontal focusing steps. Brains were imaged in autofluorescence ( $560 \pm 40$  nm excitation,  $650 \pm 50$  nm emission), BI-Cy5 compound fluorescence ( $785 \pm 25$  nm excitation and  $845 \pm 55$  nm emission) and antibody staining ( $630 \pm 15$  nm excitation and  $680 \pm 15$  nm emission) wavelengths. Data were visualized using Imaris 9.2 software (Oxford Instruments, Abingdon, UK).

### 2.8. 3D whole-brain imaging studies with BI 1820237 and BI 3005788

Chow-fed male C57BL/6J mice (Janvier Labs, France;  $n = 8$  per group) received a single subcutaneous (5 mL/kg) dose of BI 1820237 (100 nmol/kg) or BI 3005788 (100 nmol/kg), an analog of BI 1820237, labeled with a Cyanine5 fluorophore attached to the side chain of a lysine residue specifically introduced in position 10 for peptide labeling. Mice were terminated 6 h after dosing. For competition analysis, a third group of mice ( $n = 8$ ) were dosed 3 consecutive times (0–8–24 h) with BI 1820237 (100 nmol/kg, SC). One hour after the last dose of BI 1820237, mice received a single dose of BI 3005788 (100 nmol/kg, SC), and were terminated 1 h later. Terminal plasma samples were stored for optional analysis of compound exposure. Tongue tissue ( $n = 2$ ) served as a positive control for BI 3005788 binding. Following perfusion fixation, whole-brain and tongue were post-fixed in neutral-buffered formalin overnight followed by tissue clearing. Using light-sheet fluorescence microscopy (LSFM) as described above, region delineation was obtained by alignment to a digital LSFM-based mouse brain atlas. For pre-selected brain areas (CVOs, ARH), data were expressed as region-wise mean fluorescence signal intensity.

### 2.9. 3D whole-brain c-Fos imaging studies with BI 1820237 and survodutide

Diet-induced obese (DIO) male C57BL6/J mice (Janvier Labs, France) were treated acutely with either vehicle ( $n = 10$ ), BI 1820237 (8 nmol/kg,  $n = 10$ ) or survodutide (7.5 nmol/kg,  $n = 10$ ) or a combination of BI 1820237 and survodutide ( $n = 10$ ) at equimolar doses. Animals were perfused 4 h after dosing and brains were dissected. Brain samples were labeled for c-Fos and cleared according to the iDISCO+ protocol as described previously [28]. Subsequently, the samples were 3D imaged using LSFM as detailed above. Image analysis of the brain volumes included atlas mapping, detection, and quantification of c-Fos+ cells per brain region, and region-wise statistical analysis for comparing the group specific effects according to previously published methods [29].

### 2.10. Animal studies

Experimental protocols concerning the use of laboratory animals were reviewed by a federal ethics committee and approved by governmental authorities. Unless otherwise stated, the vehicle used throughout the studies was composed of 50 mM phosphate buffer pH 7.0 and 5% mannitol. The dosing of all agents was conducted at a volume of 5 mL/kg.

### 2.11. Statistical analysis

Unless stated earlier, data are presented as mean  $\pm$  SEM and were compared using a one-way ANOVA followed by Dunnett's test for multiple comparisons versus vehicle. Comparisons were considered significant at  $p < 0.05$ . Analyses were performed using GraphPad 9 statistical software (GraphPad Software). For the regression-based interaction study, the estimated parameters are provided as point estimates (e.g.,  $E_{max}$ ,  $ED_{50}$ ). Analyses were performed using the 'optimx' function in R (version 2023–10.21). Plotting of the results was performed with the ggplot2 package (version 3.5.0).

Statistical analysis of the c-Fos+ cells and accumulated signal intensity was performed by fitting a negative binomial generalized linear model (GLM) to the counts of 438 atlas-defined brain regions, for every study group. For each GLM, a Dunnett's test was performed. Statistical analysis was conducted using R (R Project for Statistical Computing) packages

MASS, multcomp, lmer, and car. All significantly regulated regions were validated to ensure that significance was not achieved due to overly influential datapoints (based on Cook's distance metric), and that the signal was not originating from the spillover of neighboring regions.

## 3. RESULTS

### 3.1. Chemical structure and pharmacokinetic profile of BI 1820237

BI 1820237 is a 34-amino-acid peptide optimized for high affinity and functional potency at the NPY2 receptor, and for selectivity against the NPY1, NPY4, and NPY5 receptors (Figure 1A). BI 1820237 is lipidated with a C18 diacid, which is attached to a lysine in position 7 (PYY derived numbering) via a flexible linker consisting of 2 oligoethylene-glycol (OEG) units and a gamma-glutamate (gGlu) residue. Lipidation results in increased albumin binding and an extended terminal half-life. Upon subcutaneous injection of BI 1820237 in animals, mean residence times of 18 h and 103 h and  $T_{max}$  values of 3 h and 32 h were obtained in mice and dogs, respectively (Supplementary Table 1), suggesting potential for once-weekly dosing frequency in humans [30]. All relevant structural features of the molecule (the amino acid sequence, the position and type of linker, and the fatty acid half-life extension) were subject to optimization to derive BI 1820237 with the desired profile, which included high solubility and chemical stability at neutral pH. BI 3005788 is an analog of BI 1820237, labeled with a Cyanine5 fluorophore attached to the side chain of a lysine residue specifically introduced in position 10 for peptide labeling.

### 3.2. BI 1820237 is a potent, selective, NPY2R agonist *in vitro*

BI 1820237 binds to the human NPY2 receptor with high sub-nanomolar affinity ( $K_i$  0.82 nM). This was comparable to the affinity determined for the endogenous ligand PYY3–36 ( $K_i$  0.51 nM; Figure 1B), in accordance with previously reported literature [14,31]. BI 1820237 selectively binds to the human NPY2R (and similarly to mouse NPY2R, see Supplementary Table 2), while no binding was detected for human NPY subtypes 1 and 4 (up to 1  $\mu$ M), and 5 (up to 200 nM; Figure 1B). The high affinity of BI 1820237 for the human NPY2R correlated with its high functional potency to lower forskolin stimulated cAMP in HEK293 cells recombinantly expressing human NPY2R with an  $EC_{50}$  of 0.19 nM. This was comparable to the potency of human PYY3–36 with an  $EC_{50}$  of 0.63 nM (Figure 1C). BI 3005788, the Cyanine5 fluorophore labeled analog of BI 1820237, demonstrated a potency similar to BI 1820237 with an  $EC_{50}$  of 0.90 nM in the cAMP assay (Figure 1C). The circulating half-life of BI 1820237 and BI 3005788 was optimized by fatty diacid acylation, which mediates albumin binding [32]. The impact of the half-life extension on functional potency was assessed in the absence (0.5%) and presence (100%) of human plasma in a CRE-Luc assay. Compared with the native peptide hormone PYY3–36 that is similarly active at low and high plasma concentrations (0.18 and 0.27 nM potency in 0.5% and 100% plasma, respectively), BI 1820237 showed a potency shift in the presence of human plasma with an  $EC_{50}$  of 0.18 nM–2.34 nM in 0.5% and 100% human plasma, respectively. The half-life extension was associated with a  $\sim$ 13-fold potency shift for BI 1820237, attributed to a lower free fraction (fraction unbound) in the presence of 100% human plasma, suggesting a high binding affinity for human serum albumin. BI 3005788, the Cyanine5 fluorophore-labeled analog of BI 1820237, demonstrated a potency similar to BI 1820237 with an  $EC_{50}$  of 0.90 nM in the cAMP assay and 100% human plasma (Figure 1C, Fig. S7). However, a lower potency shift with an  $EC_{50}$  of 0.74 nM in

## A

Peptide	N-term	1	2	3	4	5	6	7	8	9	10	11	12	13	14	15	16	17	18	19	20	21	22	23	24	25	26	27	28	29	30	31	32	33	34	C-term
Human PYY3-36	H	I	K	P	E	A	P	G	E	D	A	S	P	E	E	L	N	R	Y	Y	A	S	L	R	H	Y	L	N	L	V	T	R	Q	R	Y	NH <sub>2</sub>
BI 1820237	Iso Val	A	P	A	K*	P	E	E	D	A	S	P	E	E	I	Q	R	Y	Y	V	S	L	R	H	Y	Y	N	W	L	T	R	Q	R	Y	NH <sub>2</sub>	

## B

	Human NPY1R K <sub>i</sub> in nM (pIC <sub>50</sub> ±SD; n)	Human NPY2R K <sub>i</sub> in nM (pIC <sub>50</sub> ±SD; n)	Human NPY4R K <sub>i</sub> in nM (pIC <sub>50</sub> ±SD; n)	Human NPY5R K <sub>i</sub> in nM (pIC <sub>50</sub> ±SD; n)
PYY(3-36)	2.62 (8.58±0.11; 3)	0.51 (9.19±0.12; 3)	n.d.	4.21 (8.29±0.35; 3)
BI 1820237	>1000 (<3; 3)	0.82 (9.09±0.06; 3)	>1000 (<3; 3)	196 (6.62±0.26; 4)
PP	n.d.	n.d.	0.060 (10.24±0.08; 3)	n.d.

## C

	Human NPY2R cAMP	Human NPY2R Cre_Luciferase		
	EC <sub>50</sub> in nM (±SD; n)	Human Plasma EC <sub>50</sub> in nM (±SD; n)		Plasma Shift
		0.5%	100%	
PYY(3-36)	0.63 (±0.14; 2)	0.18 (±0.02; 5)	0.27 (±0.07; 6)	1.5
BI 1820237	0.19 (±0.05; 3)	0.18 (±0.06; 11)	2.34 (±0.53; 13)	13
BI 3005788	0.90 (-; 1)	0.74 (-; 1)	1.55 (-; 1)	2.1

**Figure 1: Structural properties and pharmacokinetic profile of BI 1820237.** A) Peptide sequence of human PYY3–36 and BI 1820237. K\* shows the C18 diacid lipidated lysine. B) Affinity of BI 1820237 to human NPY1R, NPY2R, NPY4R, and NPY5R compared with PYY3–36 and PP were investigated by competitive binding assays using membrane preparations from cells recombinantly expressing each receptor. Calculation of the affinity constant K<sub>i</sub> was performed according to the Cheng–Prusoff equation  $K_i = IC_{50}/(1 + [S])/K_m$ . C) Potency of BI 1820237, at the human NPY2R based on cAMP and luciferase induction in CRE-Luc cells in the presence of 0.5% and 100% human plasma. CRE-Luc, cAMP response element-luciferase; EC<sub>50</sub>, half-maximal effective concentration; IC<sub>50</sub>, half-maximal inhibitory concentration; NPYR, neuropeptide Y receptor; pIC<sub>50</sub>, negative log IC<sub>50</sub>; PP, pancreatic polypeptide; PYY3–36, polypeptide Y.

0.5% and 1.6 nM in 100% plasma, respectively, was noted. In conclusion, data from the cAMP and CRE-Luc assays showed that fluorophore labeling of BI 1820237 did not cause a loss in activity due to the Cyanine5 fluorophore.

### 3.3. A single dose of BI 1820237 reduces food intake and inhibits gastric emptying

The acute potency of BI 1820237 to engage the NPY2R was assessed in lean mice by determining the reduction of food intake and the inhibition of gastric emptying after single dosing. The primary aim for the doses investigated was to characterize the acute effects of BI 1820237 in lowering food intake and delaying gastric emptying to provide efficacious exposures (EC<sub>50</sub> and E<sub>max</sub>) for this clinical development

candidate to inform pre-Investigational New Drug studies, such as acute safety pharmacology studies and toxicology investigations, to derive safe starting doses and dose-multiples for a single-ascending phase I clinical trial in healthy volunteers. The potency and efficacy of BI 1820237 to inhibit food intake over 24 h was dose-dependent with an ED<sub>50</sub> of 14 nmol/kg and E<sub>max</sub> of ~85% at the maximal tested dose of 100 nmol/kg BI 1820237 (Figure 2A; EC<sub>50</sub> of 11 nM, Fig. S1a). Gastric emptying was assessed by change in acetaminophen exposure up to 4 h post-dosing (around T<sub>max</sub> for BI 1820237). Upon single dose injection of BI 1820237, gastric emptying was reduced by up to 35% (E<sub>max</sub>) with an ED<sub>50</sub> of ~2 nmol/kg (Figure 2B–D; EC<sub>50</sub> of ~8 nM, Fig. S1b). Glucose excursion measured in the same experiment (Figure 2E,F) was not affected by BI 1820237.

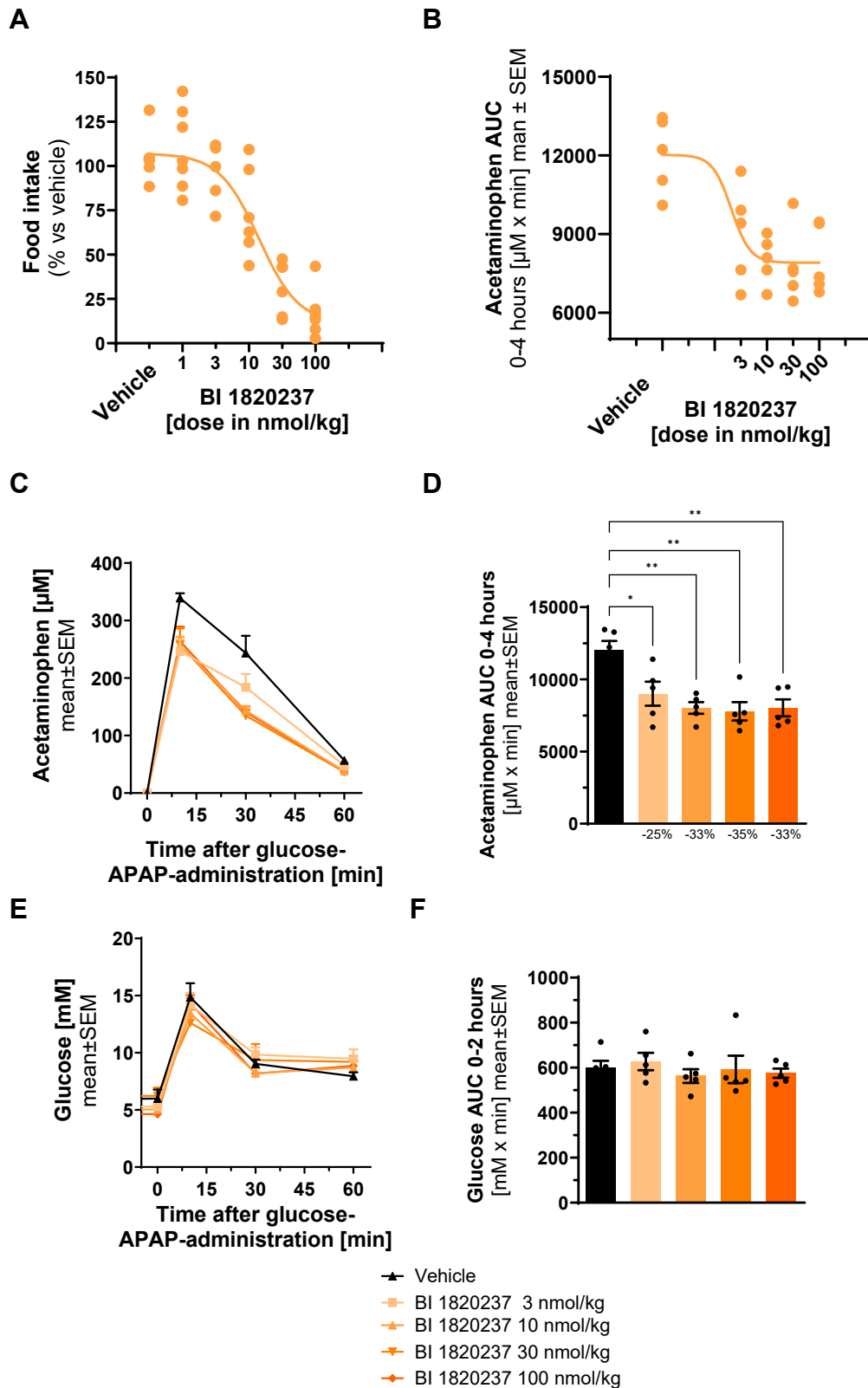


**Figure 2: NPY2R receptor engagement by BI 1820237 to reduce food intake and gastric emptying in lean animals after single dosing.** A–F) Dose-dependent effect of BI 1820237 on food intake (A), gastric emptying (B–D), and glucose clearance (E,F). The ED<sub>50</sub> for BI 1820237 to reduce food intake and gastric emptying was calculated by linear regression analysis using one-way ANOVA followed by a Dunnett's test for multiple comparisons versus vehicle. \* $p < 0.05$ , \*\* $p < 0.01$ . APAP, acetaminophen; AUC, area under the curve; ED<sub>50</sub>, half-maximal effective dose; SEM, standard error of mean.

### 3.4. Subchronic treatment with BI 1820237 transiently reduced food intake with no effect on bodyweight in DIO mice

The effect of repeated treatment with BI 1820237 on food intake and bodyweight was assessed in DIO mice. Doses used to investigate the pharmacodynamic responses in this disease-related model upon multiple dosing ranged from 3 to 100 nmol/kg. Doses were chosen to cover doses below the ED<sub>50</sub> up to the E<sub>max</sub>, which had been established for the effect of BI 1820237 to acutely reduce food intake upon single dosing in lean mice. Animals were injected once daily with 3, 10, 30, or 100 nmol/kg of BI 1820237 over a 4-week period. On Day 1, 24 h post-dosing, BI 1820237 dose-dependently reduced food intake by 18%, 59%, 71%, and 56% for the 3, 10, 30, and 100 nmol/kg doses, respectively. There was no change in food intake in the vehicle group. After 4–5 days of dosing, the food intake in the groups treated with 3, 10, and 30 nmol/kg of BI 1820237 returned to the level of the vehicle-treated group, while the food intake in the group repeatedly injected with the 100 nmol/kg dose of BI 1820237 was higher than the food intake in the vehicle group (Figure 3A). At the end of the study, the vehicle group gained ~7% of bodyweight (from 45 g to 48 g). At a dose of 30 nmol/kg, BI 1820237 non-significantly reduced bodyweight by 2% (Figure 3B), with no effect seen with other doses at the end of the study (Figure 3B). The maximal bodyweight-lowering effect of BI 1820237 was observed with the 30 nmol/kg dose at Day 5 of dosing, with a reduction of 9%. In summary, BI 1820237 caused a dose-dependent reduction of food intake during the first 3 days of dosing, returning to vehicle control thereafter. This transient reduction in food intake did not translate into a bodyweight-lowering efficacy after 4 weeks of daily dosing.

### 3.5. BI 1820237 shows greater bodyweight-lowering efficacy in DIO mice when co-administered with survodutide

The effect of BI 1820237 in combination with the GCGR/GLP-1R dual agonist survodutide on food intake and bodyweight was investigated in DIO mice. The doses selected for BI 1820237 were based on the rationale that there would be synergistic weight loss when combining a NPY2R with a GLP-1R agonist [21]. Therefore, doses of 1, 3, and 10 nmol/kg BI 1820237 were chosen, which were equal to or lower than the ED<sub>50</sub> for acute food intake reduction and inhibition of gastric emptying, to study the potential synergistic body weight lowering efficacy in combination with a stable dose of 7.5 nmol/kg of survodutide [33]. For BI 1820237 at doses of 1, 3, and 10 nmol/kg, a dose-dependent reduction in food intake by 16%, 38%, and 58% was observed 1 day after dosing, respectively, with the vehicle group showing a stable food intake during the study. Survodutide at 7.5 nmol/kg showed a 43% reduction in food intake 1 day after dosing. When doses of 1, 3, and 10 nmol/kg of BI 1820237 were combined with 7.5 nmol/kg survodutide, food intake was reduced by 58%, 64%, and 76% 1 day after dosing, respectively (Figure 3C; Fig. S1c). After 28 days of treatment, survodutide at a dose of 7.5 nmol/kg lowered bodyweight by 21% compared with the vehicle group (17% versus baseline). Co-administration of 1 nmol/kg BI 1820237 with survodutide led to a bodyweight-lowering efficacy of 26% compared with vehicle group and 5% compared with survodutide, reaching statistical significance ( $p < 0.001$ ; Figure 3D). Administration of BI 1820237 at doses of 3 and 10 nmol/kg in combination with 7.5 nmol/kg survodutide resulted in a bodyweight-lowering efficacy beyond 25%, comparable to animals that were fed a chow diet (Fig. S1d). The food intake and associated bodyweight-lowering efficacy for these two combination groups achieved or exceeded the allowance defined in the animal welfare license. Therefore, these two groups were not included in any further analysis. Food intake for different dose combinations of

BI 1820237 (0.3 nmol/kg–30 nmol/kg) and survodutide (3 nmol/kg–20 nmol/kg) is shown in Fig. S2a–c.

Treatment with 1 nmol/kg BI 1820237 did not reduce the weight of the epididymal adipose tissue compared with the vehicle group. Survodutide and BI 1820237 combination reduced the weight of the epididymal adipose tissue significantly ( $p < 0.0001$ ) compared with vehicle (Figure 3E), however combination treatment did not demonstrate a significant effect compared with survodutide-treated animals (Figure 3E). Plasma triglyceride concentrations were unaffected by BI 1820237, survodutide, and the combination thereof (Figure 3F). In contrast, liver triglycerides were significantly ( $p < 0.0001$ ) reduced by survodutide and its combination with BI 1820237 but not by BI 1820237 alone (Figure 3G). Fat mass, lean mass, and laboratory values for different dose combinations of BI 1820237 (0.3 nmol/kg–30 nmol/kg) and survodutide (3 nmol/kg–20 nmol/kg) are shown in Fig. S2d–l.

In addition to the treatment of DIO mice with a combination of survodutide and BI 1820237, we investigated whether BI 1820237 in addition to a stable dose of survodutide (8 days of daily dosing) would reduce food intake and bodyweight to the extent of the co-administration of survodutide and BI 1820237. Survodutide at a dose of 7.5 nmol/kg reduced food intake up to 10% after 28 days with a maximal efficacy of 40% at Day 4 of dosing compared with the vehicle group (Figure 4A). Co-administration of 1 and 3 nmol/kg BI 1820237 with survodutide dose-dependently reduced food intake by 68% and 59%, respectively around Day 4 of treatment (Figure 4A). When 1 and 3 nmol/kg BI 1820237 was added after 8 days of daily dosing with survodutide, food intake was maximally reduced by 53% and 56% at Day 11, 3 days after the start of BI 1820237 co-administration (Figure 4A). When compared with the vehicle group, co-administration of BI 1820237 with 7.5 nmol/kg survodutide, either from the start or after 8 days of survodutide dosing, resulted in bodyweight-lowering efficacies of 25% and 30%. This was significantly greater (between  $p < 0.01$  and  $p < 0.0001$ ) compared with survodutide treatment alone, which achieved a 17% bodyweight-lowering efficacy (Figure 4B,C).

Body composition analysis by MRI demonstrated a fat mass of 18% in vehicle-treated DIO mice, which was reduced to 12% with 7.5 nmol/kg of survodutide. Co-administration of 1 nmol/kg and 3 nmol/kg BI 1820237 with survodutide resulted in a further, significant loss in fat mass of up to 8%, when compared with vehicle after 28 days of dosing (Figure 4D). This additional reduction in body fat was independent of the treatment regimen with BI 1820237. Lean mass was significantly increased in the DIO vehicle group compared with the chow group. No significant change in lean mass was observed in animals treated with survodutide alone. Co-administration of survodutide with 3 nmol/kg BI 1820237 at study start or with 1 nmol/kg at Day 8, was associated with a loss of lean mass, which reached statistical significance. However, the lean mass in DIO mice treated with BI 1820237 and survodutide was not significantly different from chow group animals (Figure 4E).

### 3.6. The combination of BI 1820237 with survodutide provides synergistic bodyweight-lowering efficacy in DIO mice

For detailed characterization of the added bodyweight-lowering efficacy observed in DIO mice treated with a combination of BI 1820237 and survodutide compared to animals treated with survodutide alone, a novel regression-based study design was applied. This analysis aimed to provide an in-depth description of the pharmacology of triple agonism at the glucagon, GLP-1, and NPY2 receptors. The model was intended to provide dose and exposure rationale for BI 1820237 when

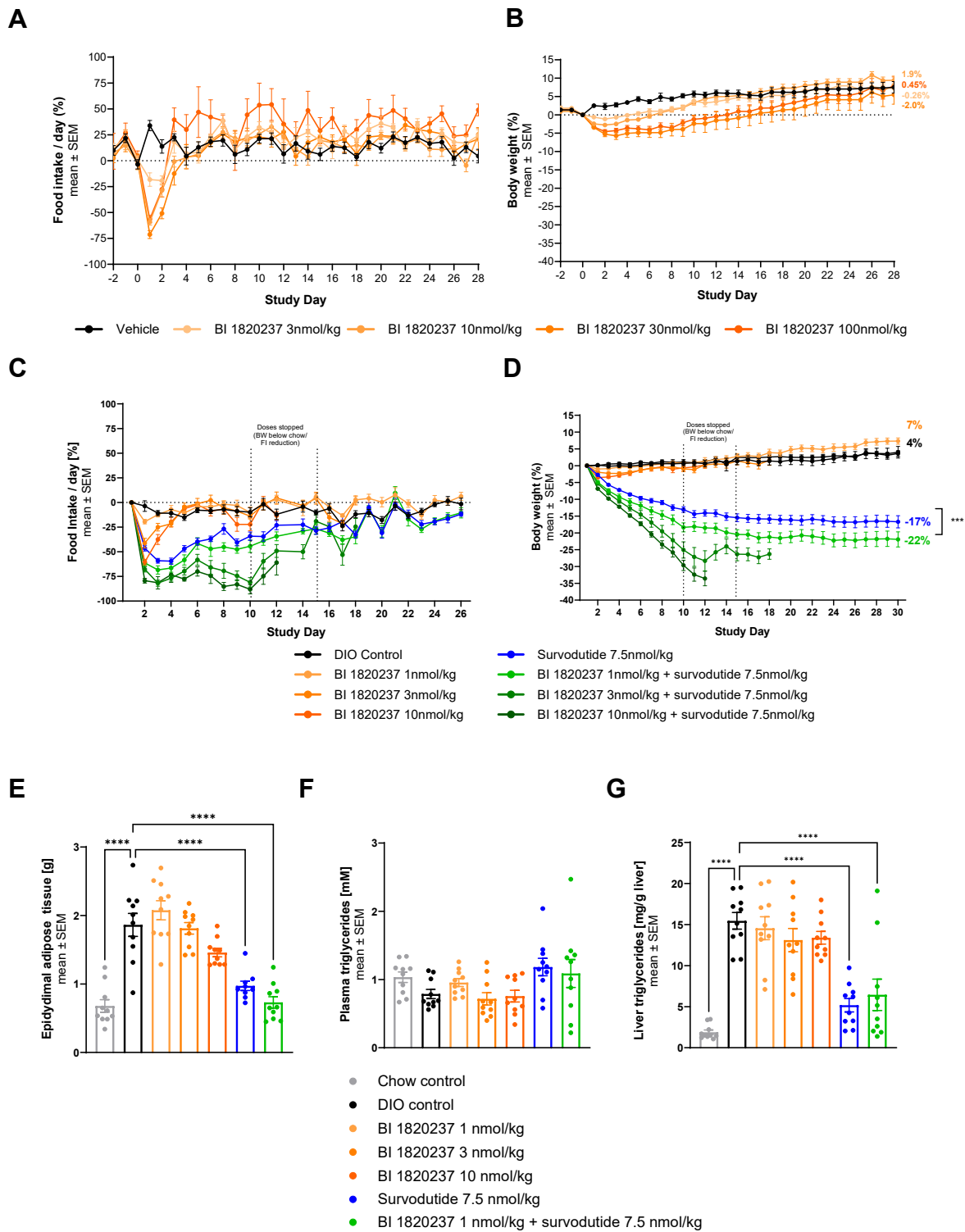


**Figure 3: Daily dosing of BI 1820237 shows a transient reduction in food intake and bodyweight and provides a more-than-additive bodyweight-lowering efficacy in combination with survodutide in diet-induced obese mice.** A–B) The effect of repeated dosing of BI 1820237 on food intake (A) and bodyweight (B) across the study period. C–D) The effect of repeated dosing of BI 1820237, survodutide, and the combination thereof on food intake (C) and bodyweight (D) across the study period. The food intake of the treated groups was normalized (in %) to the average food intake of the group receiving vehicle. E–G) The effect of repeated dosing of BI 1820237, survodutide, and the combination thereof on epididymal adipose tissue (E), plasma triglycerides (F), and liver triglycerides (G) at study end. <sup>a</sup>For BI 1820237 3 nmol/kg and 10 nmol/kg + survodutide 7.5 nmol/kg dosing was discontinued as bodyweight reduction exceeded the allowance defined in the animal welfare license. \*\*\**p* < 0.001, \*\*\*\**p* < 0.0001. BW, bodyweight; DIO, diet-induced obese; FI, food intake; SEM, standard error of mean.

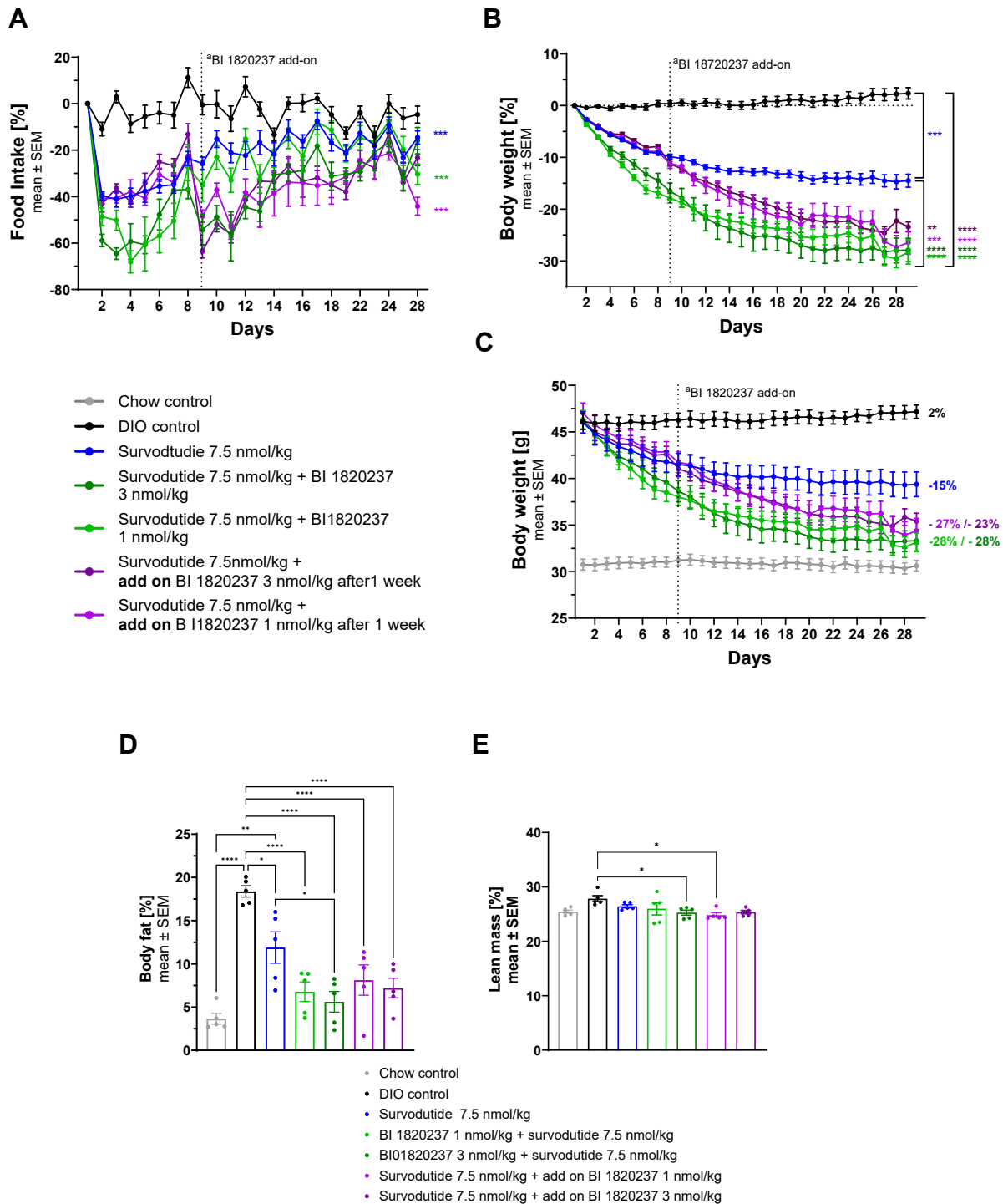


**Figure 4: BI 1820237 added to a stable dose of survodutide provides a more-than-additive bodyweight-lowering efficacy compared with survodutide alone in diet-induced obese mice.** A–C) The effect of survodutide, BI 1820237 in combination with survodutide, and BI 1820237 added after 8 days of daily survodutide dosing on food intake (A), change in bodyweight % (B), and absolute change in bodyweight (C). The food intake of the treated groups was normalized (in %) to the average food intake of the group receiving vehicle. D–E) The effect of survodutide, BI 1820237 in combination with survodutide, and BI 1820237 added after 8 days of daily survodutide dosing on body fat (D) and lean mass (E). <sup>a</sup>Dashed line denotes the addition of BI 1820237 on Day 9, after 8 days of daily survodutide.

\* $p < 0.05$ , \*\* $p < 0.01$ , \*\*\* $p < 0.001$ , \*\*\*\* $p < 0.0001$ . DIO, diet-induced obese; SEM, standard error of mean.

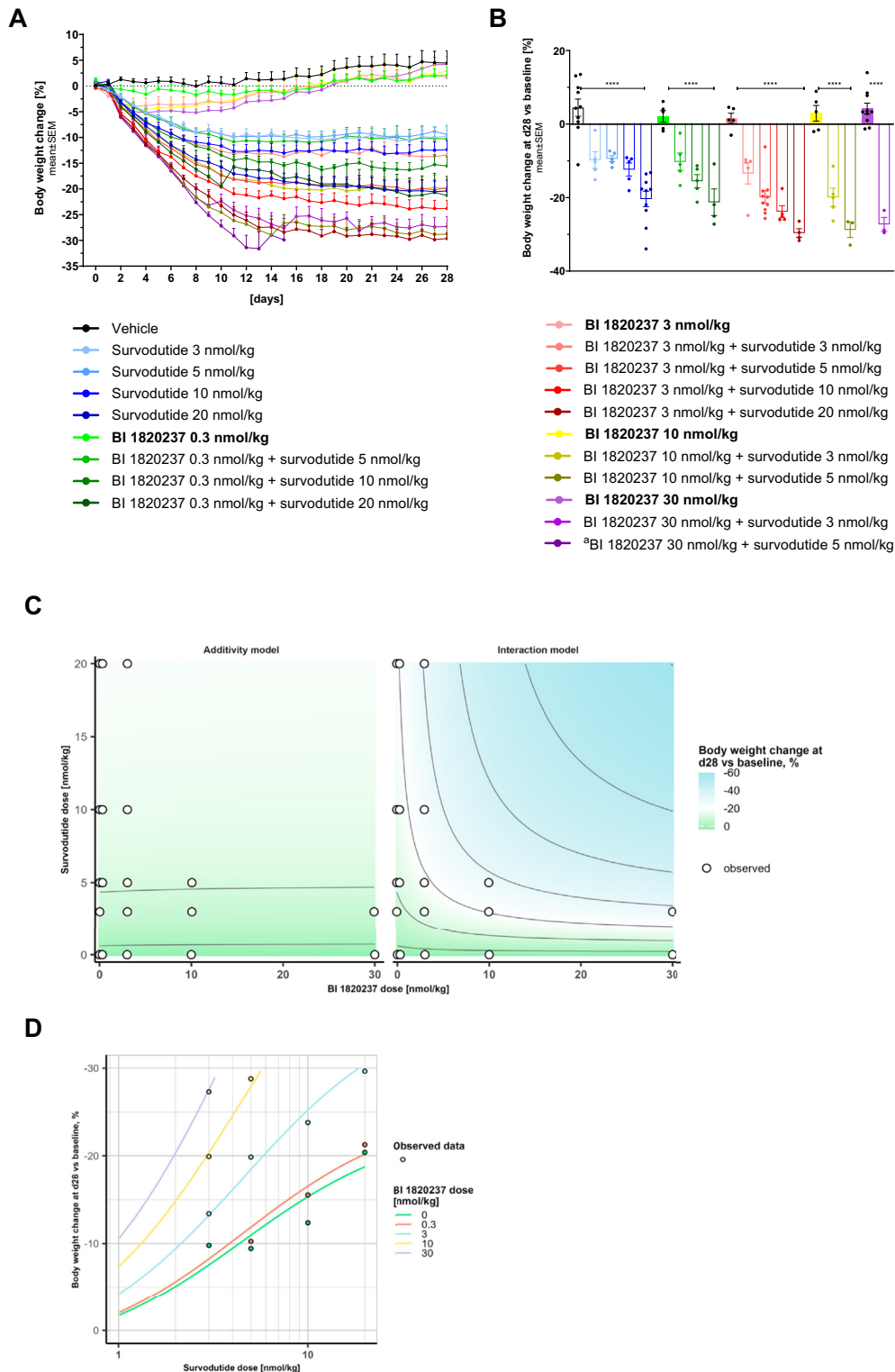


**Figure 5: The combination of BI 1820237 and survodutide provides synergistic bodyweight-lowering efficacy in diet-induced obese mice.** A) The effect of BI 1820237, survodutide, and the combination thereof on bodyweight. B) Change in bodyweight versus baseline at Day 28 following dosing with BI 1820237 and BI 1820237 in combination with survodutide. C) Study design and model-derived bodyweight loss heatmap for BI 1820237 in combination with survodutide. Left Panel: model-derived bodyweight loss based on “additivity model”. Right panel: model-derived bodyweight loss based on final “interaction model”. White points indicate the dosing regimens included in the study design. D) Dose–response profiles of survodutide when combined with different doses of BI 1820237. Lines: “interaction model”-derived dose–response profiles. Points: observed body weight at d28 (mean of  $n = 5$  or  $n = 10$ ). <sup>a</sup>Dosing group stopped at Day 15 as bodyweight reductions exceeded the allowance defined in the animal welfare license. \*\*\*\* $p < 0.0001$ . D28, Day 28; SEM, standard error of mean.

combined with survodutide to support clinical interpretation of pharmacodynamic responses, specifically food intake reduction and nausea and emesis, both related to GLP-1R and NPY2R agonism. Gaining a thorough understanding of the exposure-response relationship could leverage the clinical benefit of synergistic weight loss while mitigating risks of nausea and emesis, as has been suggested for other GLP-1 and NPY2R dual agonists [34]. The study design and respective analysis of the bodyweight-lowering efficacies supported the conclusion of a statistically significant synergistic effect by the NPY2R agonist BI 1820237 when combined with the GCGR/GLP-1R dual agonist survodutide (Figure 5A–B). Here, the survodutide-mediated bodyweight loss was increased by up to 2.65-fold across doses with an ED<sub>50</sub> of 11.7 nmol/kg of BI 1820237. An interaction model-based bodyweight loss heatmap illustrates the synergistic effects in comparison to additive pharmacology (Figure 5C). Due to this synergy, even doses of BI 1820237 as low as 1–3 nmol/kg provided synergistic effects in combination with survodutide (Figure 5D).

### 3.7. 3-D whole-brain imaging studies with BI 1820237 and BI 3005788

BI 3005788 was designed as a Cyanine5 fluorophore analog of BI 1820237 to investigate the site of action for BI 1820237. The *in vitro* potency of BI 3005788 was comparable with BI 1820237 (Figure 1C). Upon acute dosing in lean mice, BI 3005788 at 100 nmol/kg lowered food intake up to 6 h post-dosing to a degree that was comparable with BI 1820237 dosed at 30 nmol/kg (Fig. S3a–b). Upon intravenous dosing at 100 and 200 nmol/kg, fluorophore signals were apparent 2 h post-dosing in the median eminence of the hypothalamus (ME), arcuate nucleus of the hypothalamus (ARH), and the capillary system of choroid plexus when compared with vehicle-treated animals (Fig. S3c–d). Analysis of murine lingual epithelia layer, which abundantly expresses NPY receptors, particularly the NPY2R, suggested specific labeling of NPY2R by BI 3005788 [35,36]. BI 3005788 labeling was reduced upon prior dosing of BI 1820237 (Fig. S6), suggestive of NPY2R-specific binding and labeling by BI 3005788 (Figure 6A–E; Fig. S4a). In the mouse brain, BI 3005788 signal accumulated in 5 circumventricular organs (CVOs; subfornical organ [SFO], area postrema [AP], ME, the choroid plexus in the lateral and fourth ventricle, and ARH; Figure 6C). These areas reside outside of the blood–brain barrier. BI 1820237 pre-dosing did not significantly influence BI 3005788 signal accumulation in the SFO, ME, and choroid plexus VL/4V, suggesting non-specific binding of BI 3005788 in these CVO regions (Figure 6C; Fig. S4b). Notably, pre-dosing with BI 1820237 significantly reduced BI 3005788 signal in the AP and ARH, areas exhibiting high NPY2R expression (Figure 6A–E).

### 3.8. BI 1820237 synergistically increases c-Fos activity when co-administered with survodutide

c-Fos labeling was performed to demonstrate that the synergy of GLP-1R and NPY2R agonism can not only be described pharmacologically (bodyweight-lowering efficacy) but also mechanistically by applying whole-brain imaging for c-fos as a marker for neuronal activity. A systematic analysis of bodyweight-lowering mechanisms applying this methodology provided evidence that various drug classes act via discrete brain regions and neurocircuits, supporting c-fos labeling as a method of choice for mode of action studies [29]. To test if the combination of BI 1820237 and survodutide impacts neuronal activity in appetite regulation brain regions, DIO mice were injected with either vehicle, BI 1820237 (8 nmol/kg), survodutide (7.5 nmol/kg), or a combination of these equimolar doses. Four hours after dosing, the brains were removed and analyzed for whole-brain c-Fos expression.

In animals dosed with BI 1820237 alone, little or no difference was observed compared with vehicle (Figure 7A,B). In the survodutide group, c-Fos expression in the central nucleus of the amygdala (CEA) was significantly upregulated compared with the vehicle groups (Figure 7A,B; Fig. S5a–c). In animals co-administered with BI 1820237 and survodutide, c-Fos was significantly upregulated in the parabrachial nucleus (PB), NTS, and dorsal motor nucleus of the vagus nerve (DMX), in addition to the CEA and the paraventricular nucleus of the thalamus (PVT) (Figure 7A,B; Fig. S5a–d). When comparing the total c-Fos counts in the CEA across the 4 groups, the average number of c-Fos positive cells was 10.6 (SEM ± 3.61) in the vehicle group, 19.6 (SEM ± 4.05) in the BI 1820237 group, 60.5 (SEM ± 13.2) in the survodutide group, and 137 (SEM ± 23.4) when BI 1820237 and survodutide were combined (Figure 7C). In the NTS, the number of c-Fos positive cells in the single-dosed animals was the same as in the vehicle group, while there was a 20-fold increase (from 3 to 60) when BI 1820237 and survodutide were dosed in combination (Figure 7D). The same was true in the DMX where combination treatment led to a 24-fold increase in c-Fos detected cells (from 1 to 24; Figure 7E). In the PB, the number of c-Fos positive cells with the combination of BI 1820237 and survodutide increased from 20 to 53 cells when compared to vehicle and single dosed animals (Figure 7F).

## 4. DISCUSSION

BI 1820237 is a synthetic peptide agonist for the human NPY2R with high affinity and functional activity. The pharmacokinetic profile and the physicochemical properties of BI 1820237 were optimized to support a once-weekly dosing regimen in a fixed-dose combination by co-formulation with the GCGR/GLP-1R dual agonist survodutide. The pharmacokinetic profile was optimized by acylation to reduce renal clearance and provide resistance to proteolytic cleavage. Peptide acylation represents a clinically validated approach to increase *in vivo* half-life by promoting high-affinity albumin binding [37]. Chemical modifications to the length of the fatty acids, linker type, and sites of attachment not only affect the physicochemical properties of a peptide, but also change the affinities to the target receptors and plasma proteins [38–40], and most importantly, the pharmacology of such modified peptide hormones [39–42]. *In vitro* characterization of BI 1820237 receptor binding and functional activity demonstrated high affinity and functional potency that is comparable with the endogenous NPY2R agonist PYY(3–36). As a surrogate for BI 1820237 activity in plasma, considering that free and plasma bound drug concentrations are difficult to measure for acylated modified peptides, the effect of the C18-diacid on receptor potency was determined in a CRE-Luc assay in the presence of low (0.5%) and high (100%) human plasma concentration. In this assay, plasma concentrations did not affect PYY(3–36) potencies corresponding with a plasma activity shift of 1.5, supporting the conclusion that the native peptide hormone does not significantly bind to plasma proteins. In contrast, and as expected, the high plasma protein binding property of BI 1820237 resulted in a 13-fold shift in potency from 0.18 nM to 2.34 nM in 0.5% and 100% human plasma, respectively, which is indicative of a low free fraction of the drug in the presence of plasma proteins. *In vivo*, BI 1820237 dose-dependently reduced food intake in lean and obese animals and inhibited gastric emptying in lean, fasted animals in the acetaminophen uptake test, while no changes in glucose excursion were observed. Food intake inhibition, as an endpoint that is accumulated over the time course of 24 h, was observed at doses that inhibited gastric emptying 4 h post-dosing (near the maximal exposure of BI 1820237). These data are in concordance with investigations of PYY3–36 in non-human primates

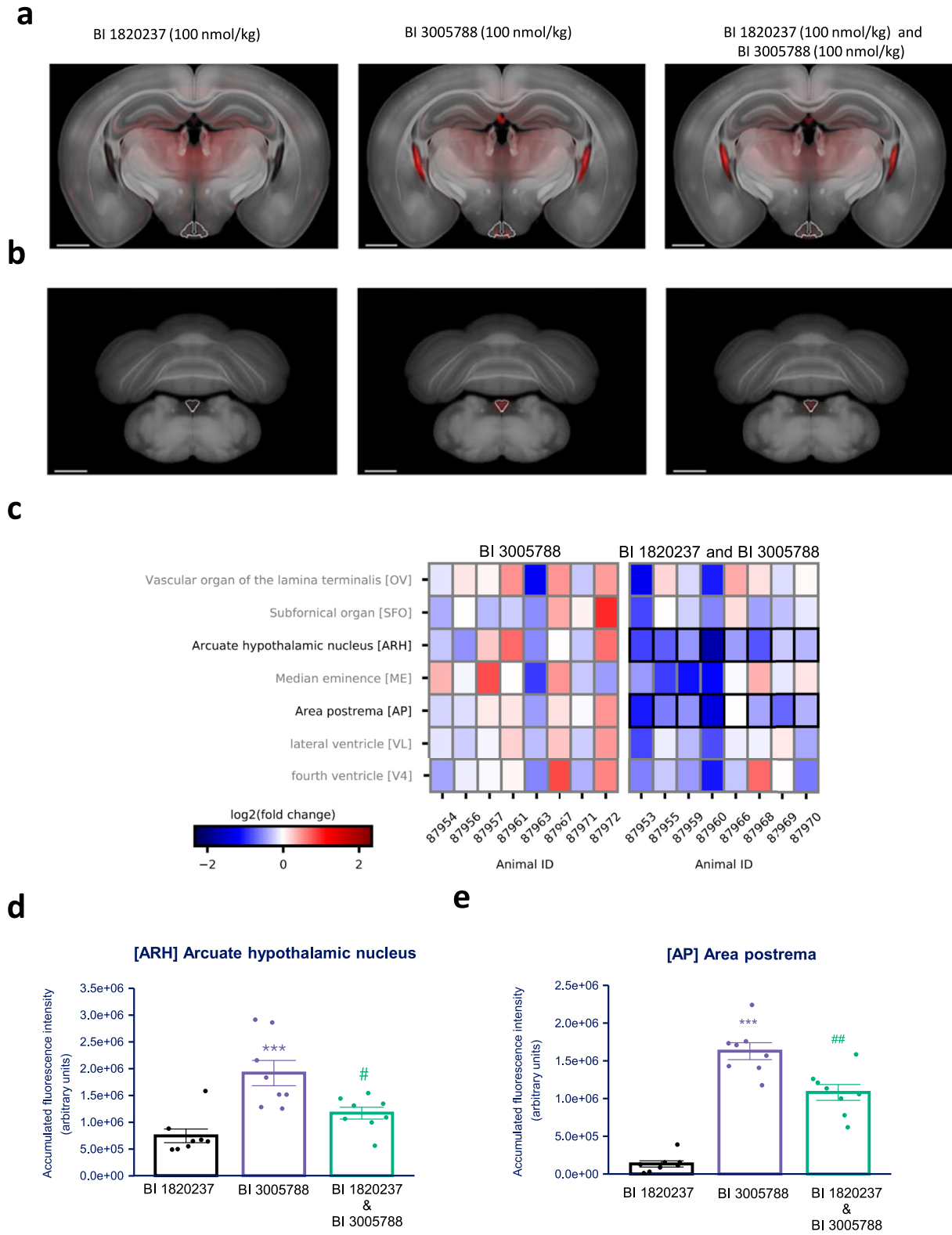


**Figure 6: BI 1820237, and the Cyanine5 fluorophore analog BI 3005788, bind to centers of the arcuate nucleus of the hypothalamus and area postrema.** A-B) Group-averaged whole brain images (coronal view) showing BI 3005788 targeting the ARH (A) and the AP (B). Fluorescence signal intensity from every light sheet imaged brain was mapped to Gubra average 3D brain volume to reconstruct group average fluorescence distribution patterns. Section is taken from the 3D reconstructed brain at the level of the ARH (A) and the AP (B). Scale bar, 1 mm. C) Heat map representing the mean log<sub>2</sub> fold-change in region-wise mean fluorescence signal intensity for 7 pre-selected CVOs for chow-fed male C57BL/6JRj mice that received either a single subcutaneous dose of BI 3005788 (100 nmol/kg) or three consecutive subcutaneous doses of BI 1820237 (100 nmol/kg), followed by a single subcutaneous dose of BI 3005788 (100 nmol/kg). D-E). Region-wise mean fluorescence signal intensity for the ARH (D) and AP (E) for BI 1820237, BI 3005788, and BI 1820237 plus BI 3005788 competition analysis dose groups. Values expressed as mean of  $n = 8 + SEM$ . Dunnett's test one-factor linear model. Region delineation was obtained by alignment to a digital LSFM-based mouse brain atlas. \* $p < 0.05$  compared with BI 3005788, \*\* $p < 0.01$  compared with BI 3005788, \*\*\* $p < 0.001$  compared with BI 1820237. ARH, arcuate nucleus of the hypothalamus; AP, area postrema; CVO, circumventricular organs; LSFM, light sheet fluorescence microscopy; SC, subcutaneous; SEM, standard error of mean.

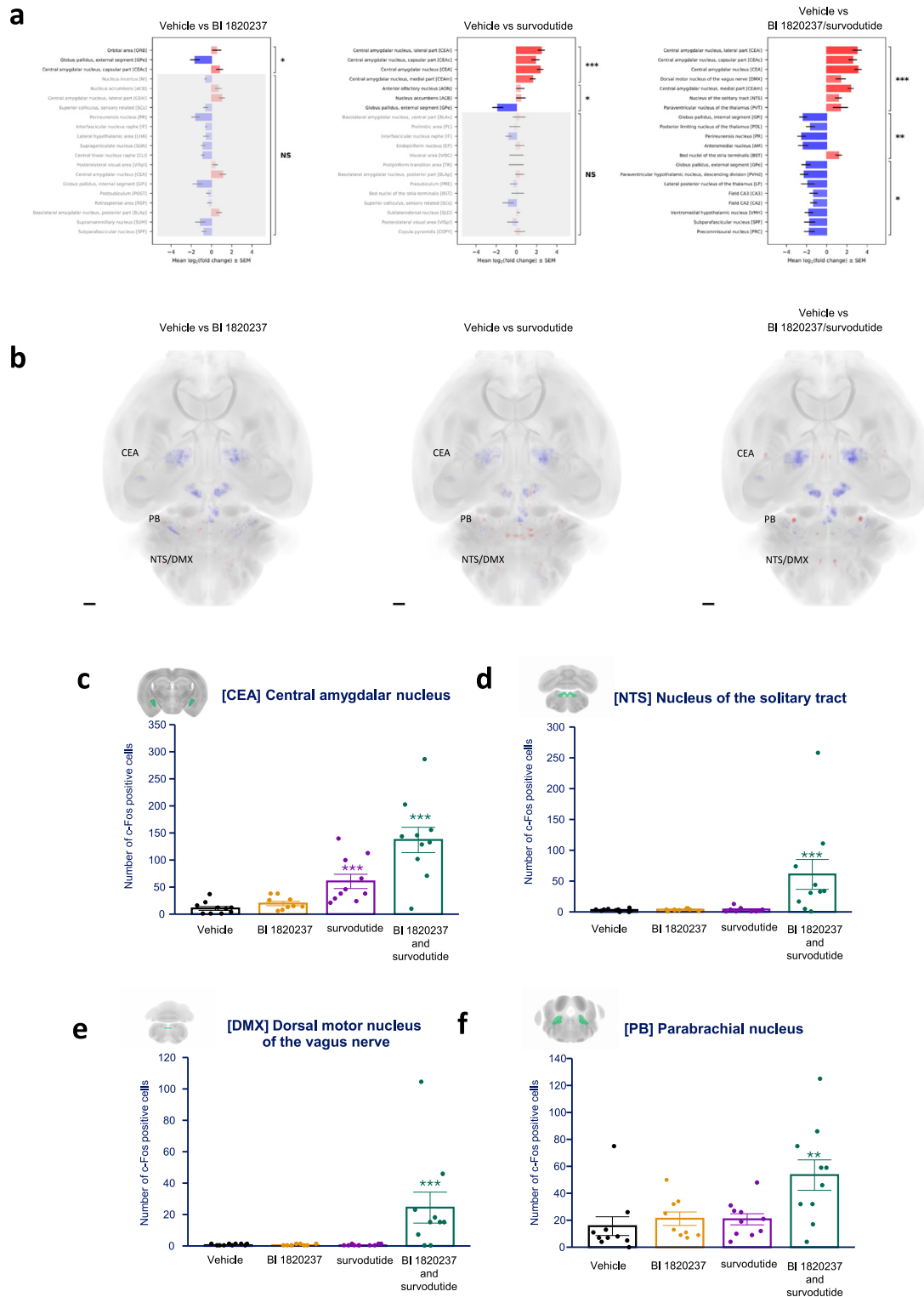


**Figure 7: BI 1820237 and survodutide in combination synergistically increase c-Fos activity in the central nervous system.** A) Brain regions and the mean log<sub>2</sub> fold-change in the number of c-Fos positive cells in these regions in DIO mice that received either BI 1820237 (8 nmol/kg), survodutide (7.5 nmol/kg), or combination BI 1820237 and survodutide, compared with vehicle. B) Up (red) and down (blue) regulation of c-Fos expression in DIO mice that received either BI 1820237 (8 nmol/kg), survodutide (7.5 nmol/kg), or combination BI 1820237 and survodutide, compared with vehicle. C-F) Number of c-Fos positive cells in the CEA (C), NTS (D), DMX (E), and PB (F) of DIO mice that received either vehicle, BI 1820237 (8 nmol/kg), survodutide (7.5 nmol/kg), or combination BI 1820237 and survodutide. \**p* < 0.05, \*\**p* < 0.01, \*\*\**p* < 0.001. CEA, central amygdala nucleus; DIO, diet-induced obese; DMX, dorsal motor nucleus of the vagus nerve; NTS, nucleus of the solitary tract; PB, parabrachial nucleus; SEM, standard error of mean. (For interpretation of the references to colour in this figure legend, the reader is referred to the Web version of this article.)

[43] and humans [44], where a reduction in caloric intake, inhibition of gastric emptying, and increases in nausea and emesis were observed without significant effects on glucose homeostasis. In a cardiovascular study in cynomolgus monkeys, subcutaneous supratherapeutic doses of BI 1820237 induced emesis. However, considering the pharmacokinetic profile of BI 1820237 aiming for a minimal peak-trough variation, combined with a dose escalation regimen, might allow definition of a therapeutic window, as reported for a PYY-antibody conjugate in non-human primates [45]. We believe that the thorough preclinical investigation of BI 1820237, including the novel dose–response “interaction-model” with survodutide, supports clinical dose-selection and dose-escalation with a rationale for a therapeutic window to achieve body lowering efficacies that might be otherwise limited by gastrointestinal side effects. The outcomes of the phase I study of BI 1820237, alone and in combination with liraglutide, in healthy men with overweight or obesity reported data on nausea and emesis as well as gastric emptying inhibition suggesting that combining BI 1820237 with GLP-1R agonists may help to develop an effective, long-term treatment for people living with obesity [46]. Upon subchronic dosing in DIO mice, reductions in food intake with BI 1820237 were transient, returning to or even exceeding that of the vehicle-treated animals between Days 3 and 4 of dosing. The transient reduction of caloric intake by this NPY2R agonist did not translate into significant bodyweight-lowering efficacies after 4 weeks of dosing, which is in accordance with the pharmacology of PYY3–36 and analogs thereof when administered to mice [28,47,48]. This transient anorectic effect of NPY2R agonism might be related to receptor desensitization specific to this G $\alpha$ i-coupled receptor [49], counter-regulatory responses of the central NPY systems, which have been shown to involve the NPY5R, for example [50], or tachyphylaxis related to peripheral and central inputs as well as excitatory and inhibitory signaling via NPY2R integrated by the dorsal vagal complex [51,52]. Using BI 3005788, we were able to provide evidence that BI 1820237, that is peripherally administered, binds to NPY2Rs in the ARH and AP [53], important centers for controlling energy homeostasis and examples of the CVOs accessible by peripheral hormonal inputs [54]. These results, taken together with the c-fos data, suggest, that neuronal activation with BI 1820237 occurs in deeper areas of the brain (in particular when combined with survodutide) despite those neurocircuits not being directly accessed, as BI 1820237 does not cross the blood–brain barrier, which is similar to data reported for peptide hormone mimetics of GLP-1 and amylin [29,55,56]. In combination with the GCGR/GLP-1R dual agonist survodutide, BI 1820237 demonstrated a durable inhibition of food intake that translated into a greater bodyweight reduction than survodutide alone. Combining the pharmacology of GLP-1 with NPY2 receptor agonism has previously been shown to provide more-than-additive weight loss efficacy in preclinical models overcoming the transient food intake inhibition by NPY2R agonism [19–22]. Using whole-brain imaging analysis, we were able to demonstrate that while NPY2R agonism did not increase c-Fos immunoreactivity as previously shown [21], combining BI 1820237 with survodutide increased c-Fos labeling more than additively compared with survodutide alone. The quantitative assessment of c-Fos labeling provides a mechanistic support for the observation of a more-than-additive food intake and bodyweight-lowering efficacy seen with BI 1820237 and survodutide when combined, and confirms various studies of GLP-1 and NPY2 receptor agonist combinations [20,21,57]. Applying a regression-based analysis, the combination of BI 1820237 with survodutide was shown to provide a synergistic weight loss exceeding that of a NPY2 and GLP-1 receptor agonist combination, supporting potential dose-rationales for

clinical investigation of this combination [46]. The GCGR agonism-mediated increase in energy expenditure [58], in addition to the synergistically acting anorectic principles of GLP-1 and NPY2 receptor agonism to reduce energy intake, is considered an attractive mode of action providing durable, clinically relevant weight loss in patients with obesity.

In summary, BI 1820237 is a novel, lipidated NPY2R agonist, that in combination with survodutide achieves a synergistic bodyweight-lowering efficacy. Our data provide the scientific rationale for clinical exploration of this combination in people living with obesity [46].

## ACKNOWLEDGMENTS

BI 1820237 was licensed from Gubra. Survodutide was licensed from Zealand Pharma. Boehringer Ingelheim is solely responsible for development and commercialization of both. The authors would like to thank Urmas Roostalu, Anke Voigt, Julia Wunderlich, Carina Hertenberger, Christina Triebel, Sandra Gross, Michelle Portenhausner, Jessica Grunwald, Andrea Lorenz, Eva Bernstein, Ramona Maier-Roth, Johanna Schurer, Annette Halder, Anett Kieserling, Jürgen Jäger, Dominik Frey, Beate Fanselow, Charlotte S. Madsen, Anna-Karin Lundbaek, Søren L. Pedersen, Andreas N. Madsen, Lars Yndal, and Lisbeth Elster for their excellent technical support. Editorial support in the preparation of this manuscript was provided by Kayleigh Walker, PhD, of Envision Ignite, an Envision Medical Communications agency, a part of Envision Pharma Group, and was funded by Boehringer Ingelheim. Boehringer Ingelheim was given the opportunity to review the manuscript for medical and scientific accuracy, as well as intellectual property considerations.

## CRedit AUTHORSHIP CONTRIBUTION STATEMENT

**Robert Augustin:** Writing — review & editing, Writing — original draft, Visualization, Validation, Project administration, Investigation, Conceptualization. **Anouk Oldenburger:** Writing — review & editing, Visualization, Investigation, Formal analysis, Data curation, Conceptualization. **Tamara Baader-Pagler:** Writing — review & editing, Investigation, Formal analysis, Data curation, Conceptualization. **Tina Zimmermann:** Writing — review & editing, Investigation, Formal analysis, Data curation, Conceptualization. **Jens Borghardt:** Writing — review & editing, Formal analysis, Data curation, Conceptualization. **Jacob Hecksher-Sørensen:** Writing — review & editing, Investigation, Data curation, Conceptualization. **Angela Baljuls:** Writing — review & editing, Investigation, Data curation, Conceptualization. **Wolfgang Reindl:** Writing — review & editing, Investigation, Data curation. **Bartłomiej Krawczyk:** Writing — review & editing, Formal analysis, Data curation, Conceptualization. **Eric Martel:** Writing — review & editing, Data curation, Conceptualization. **Albert Brennauer:** Writing — review & editing, Investigation, Conceptualization. **Stefan Peters:** Writing — review & editing, Investigation. **Achim Grube:** Writing — review & editing, Investigation, Conceptualization. **Lise Biehl Rudkjaer:** Writing — review & editing, Project administration, Conceptualization. **Peter Haebel:** Writing — review & editing, Visualization, Project administration, Conceptualization.

## DECLARATION OF COMPETING INTEREST

The authors declare the following financial interests/personal relationships which may be considered as potential competing interests: This work was supported by Boehringer Ingelheim Pharma GmbH & Co KG. Robert Augustin reports a relationship with Boehringer Ingelheim Pharma

GmbH & Co KG that includes: employment. Anouk Oldenburger reports a relationship with Boehringer Ingelheim Pharma GmbH & Co KG that includes: employment. Tamara Baader-Pagler reports a relationship with Boehringer Ingelheim Pharma GmbH & Co KG that includes: employment. Tina Zimmermann reports a relationship with Boehringer Ingelheim Pharma GmbH & Co KG that includes: employment. Jens Borghardt reports a relationship with Boehringer Ingelheim Pharma GmbH & Co KG that includes: employment. Jacob Hecksher-Sørensen reports a relationship with Gubra A/S that includes: employment. Angela Baljuls reports a relationship with Boehringer Ingelheim Pharma GmbH & Co KG that includes: employment. Wolfgang Reindl reports a relationship with Boehringer Ingelheim Pharma GmbH & Co KG that includes: employment. Bartłomiej Krawczyk reports a relationship with Boehringer Ingelheim Pharma GmbH & Co KG that includes: employment. Eric Martel reports a relationship with Boehringer Ingelheim Pharma GmbH & Co KG that includes: employment. Albert Brennauer reports a relationship with Boehringer Ingelheim Pharma GmbH & Co KG that includes: employment. Stefan Peters reports a relationship with Boehringer Ingelheim Pharma GmbH & Co KG that includes: employment. Achim Grube reports a relationship with Boehringer Ingelheim Pharma GmbH & Co KG that includes: employment. Lise Biehl Rudkjaer reports a relationship with Gubra A/S that includes: employment. Peter Haebel reports a relationship with Boehringer Ingelheim Pharma GmbH & Co KG that includes: employment. RA, PH, TBP, TZ, BK, JB, EM, ABa, ABr, AG, WR are employees of Boehringer Ingelheim. AO is an employee of Novo Nordisk A/S; at the time of project initiation, AO was an employee of Boehringer Ingelheim. JHS, LBR are employees of Gubra A/S. RA, AO, ABr, SP, and PH are listed as inventors on patent(s) related to this work (owned by Boehringer Ingelheim International GmbH); they do not receive any direct financial compensation related to the patent(s). If there are other authors, they declare that they have no known competing financial interests or personal relationships that could have appeared to influence the work reported in this paper.

## DATA AVAILABILITY

Data will be made available on request.

## LEAD CONTACT

Further information and requests for resources and reagents should be directed to and will be fulfilled by the Lead Contact, Robert Augustin ([robert.augustin@boehringer-ingelheim.com](mailto:robert.augustin@boehringer-ingelheim.com)).

## MATERIALS AVAILABILITY

This study did not generate new unique reagents.

## APPENDIX A. SUPPLEMENTARY DATA

Supplementary data to this article can be found online at <https://doi.org/10.1016/j.molmet.2025.102205>.

## REFERENCES

- [1] Hales CM, Carroll MD, Fryar CD, Ogden CL. Prevalence of obesity and severe obesity among adults: United States, 2017-2018. *NCHS Data Brief*; 2020. p. 1–8.
- [2] World Health Organisation. Prevalence of obesity among adults, BMI  $\geq$  30, age-standardised estimates by WHO region. Available at: <http://apps.who.int/gho/data/view.main.REGION2480A>. [Accessed 8 August 2022].
- [3] GBD Chronic Kidney Disease Collaboration. Global, regional, and national age-sex-specific mortality for 282 causes of death in 195 countries and territories, 1980-2017: a systematic analysis for the Global Burden of Disease Study 2017. *Lancet* 2018;392:1736–88. [https://doi.org/10.1016/s0140-6736\(18\)32203-7](https://doi.org/10.1016/s0140-6736(18)32203-7).
- [4] Arnold M, Pandeya N, Byrnes G, Renehan PAG, Stevens GA, Ezzati PM, et al. Global burden of cancer attributable to high body-mass index in 2012: a population-based study. *Lancet Oncol* 2015;16:36–46. [https://doi.org/10.1016/s1470-2045\(14\)71123-4](https://doi.org/10.1016/s1470-2045(14)71123-4).
- [5] Bhaskaran K, Douglas I, Forbes H, dos-Santos-Silva I, Leon DA, Smeeth L. Body-mass index and risk of 22 specific cancers: a population-based cohort study of 5.24 million UK adults. *Lancet* 2014;384:755–65. [https://doi.org/10.1016/s0140-6736\(14\)60892-8](https://doi.org/10.1016/s0140-6736(14)60892-8).
- [6] Godoy-Matos AF, Silva Júnior WS, Valerio CM. NAFLD as a continuum: from obesity to metabolic syndrome and diabetes. *Diabetol Metab Syndr* 2020;12:60. <https://doi.org/10.1186/s13098-020-00570-y>.
- [7] Rinella ME. Nonalcoholic fatty liver disease: a systematic review. *JAMA* 2015;313:2263–73. <https://doi.org/10.1001/jama.2015.5370>.
- [8] Kyle TK, Dhurandhar EJ, Allison DB. Regarding obesity as a disease: evolving policies and their implications. *Endocrinol Metab Clin N Am* 2016;45:511–20. <https://doi.org/10.1016/j.ecl.2016.04.004>.
- [9] National Center for Health Statistics 2021. Health, United States, 2019. National Center for Health Statistics (US): Hyattsville (MD).
- [10] Jastreboff AM, Kushner RF. New frontiers in obesity treatment: GLP-1 and nascent nutrient-stimulated hormone-based therapeutics. *Annu Rev Med* 2023;74:125–39. <https://doi.org/10.1146/annurev-med-043021-014919>.
- [11] Mentlein R, Dahms P, Grandt D, Kruger R. Proteolytic processing of neuropeptide Y and peptide YY by dipeptidyl peptidase IV. *Regul Pept* 1993;49:133–44. [https://doi.org/10.1016/0167-0115\(93\)90435-b](https://doi.org/10.1016/0167-0115(93)90435-b).
- [12] Cabrele C, Beck-Sickinger AG. Molecular characterization of the ligand-receptor interaction of the neuropeptide Y family. *J Pept Sci* 2000;6:97–122. [https://doi.org/10.1002/\(SICI\)1099-1387\(200003\)6:3<97::AID-PSC236>3.0.CO;2-E](https://doi.org/10.1002/(SICI)1099-1387(200003)6:3<97::AID-PSC236>3.0.CO;2-E).
- [13] Tang T, Tan Q, Han S, Diemar A, Lobner K, Wang H, et al. Receptor-specific recognition of NPY peptides revealed by structures of NPY receptors. *Sci Adv* 2022;8:eabm1232. <https://doi.org/10.1126/sciadv.abm1232>.
- [14] Gerald C, Walker MW, Vaysse PJ, He C, Branchek TA, Weinschank RL. Expression cloning and pharmacological characterization of a human hippocampal neuropeptide Y/peptide YY Y2 receptor subtype. *J Biol Chem* 1995;270:26758–61. <https://doi.org/10.1074/jbc.270.45.26758>.
- [15] Karra E, Chandarana K, Batterham RL. The role of peptide YY in appetite regulation and obesity. *J Physiol* 2009;587:19–25. <https://doi.org/10.1113/jphysiol.2008.164269>.
- [16] Batterham RL, flytche DH, Rosenthal JM, Zelaya FO, Barker GJ, Withers DJ, et al. PYY modulation of cortical and hypothalamic brain areas predicts feeding behaviour in humans. *Nature* 2007;450:106–9. <https://doi.org/10.1038/nature06212>.
- [17] Chelikani PK, Haver AC, Reidelberger RD. Comparison of the inhibitory effects of PYY(3-36) and PYY(1-36) on gastric emptying in rats. *Am J Physiol Regul Integr Comp Physiol* 2004;287:R1064–70. <https://doi.org/10.1152/ajpregu.00376.2004>.
- [18] Alonso AM, Cork SC, Phuah P, Hansen B, Norton M, Cheng S, et al. The vagus nerve mediates the physiological but not pharmacological effects of PYY(3-36) on food intake. *Mol Metabol* 2024;81:101895. <https://doi.org/10.1016/j.molmet.2024.101895>.
- [19] Boland BB, Laker RC, O'Brien S, Sitaula S, Sermadiras I, Nielsen JC, et al. Peptide-YY(3-36)/glucagon-like peptide-1 combination treatment of obese diabetic mice improves insulin sensitivity associated with recovered pancreatic beta-cell function and synergistic activation of discrete hypothalamic and brainstem neuronal circuitries. *Mol Metabol* 2022;55:101392. <https://doi.org/10.1016/j.molmet.2021.101392>.

- [20] Lear S, Pflimlin E, Zhou Z, Huang D, Weng S, Nguyen-Tran V, et al. Engineering of a potent, long-acting NPY2R agonist for combination with a GLP-1R agonist as a multi-hormonal treatment for obesity. *J Med Chem* 2020;63:9660–71. <https://doi.org/10.1021/acs.jmedchem.0c00740>.
- [21] Kjaergaard M, Salinas CBG, Rehfeld JF, Secher A, Raun K, Wulff BS. PYY(3-36) and exendin-4 reduce food intake and activate neuronal circuits in a synergistic manner in mice. *Neuropeptides* 2019;73:89–95. <https://doi.org/10.1016/j.npep.2018.11.004>.
- [22] Schmidt JB, Gregersen NT, Pedersen SD, Arentoft JL, Ritz C, Schwartz TW, et al. Effects of PYY3-36 and GLP-1 on energy intake, energy expenditure, and appetite in overweight men. *Am J Physiol Endocrinol Metab* 2014;306:E1248–56. <https://doi.org/10.1152/ajpendo.00569.2013>.
- [23] van den Hoek AM, Heijboer AC, Corssmit EP, Voshol PJ, Romijn JA, Havekes LM, et al. PYY3-36 reinforces insulin action on glucose disposal in mice fed a high-fat diet. *Diabetes* 2004;53:1949–52. <https://doi.org/10.2337/diabetes.53.8.1949>.
- [24] van den Hoek AM, Heijboer AC, Voshol PJ, Havekes LM, Romijn JA, Corssmit EP, et al. Chronic PYY3-36 treatment promotes fat oxidation and ameliorates insulin resistance in C57BL6 mice. *Am J Physiol Endocrinol Metab* 2007;292:E238–45. <https://doi.org/10.1152/ajpendo.00239.2006>.
- [25] Loffler MC, Betz MJ, Blondin DP, Augustin R, Sharma AK, Tseng YH, et al. Challenges in tackling energy expenditure as obesity therapy: from preclinical models to clinical application. *Mol Metabol* 2021;51:101237. <https://doi.org/10.1016/j.molmet.2021.101237>.
- [26] Christoffersen B, Sanchez-Delgado G, John LM, Ryan DH, Raun K, Ravussin E. Beyond appetite regulation: targeting energy expenditure, fat oxidation, and lean mass preservation for sustainable weight loss. *Obesity* 2022;30:841–57. <https://doi.org/10.1002/oby.23374>.
- [27] Cheng Y, Prusoff WH. Relationship between the inhibition constant (K<sub>1</sub>) and the concentration of inhibitor which causes 50 per cent inhibition (I<sub>50</sub>) of an enzymatic reaction. *Biochem Pharmacol* 1973;22:3099–108. [https://doi.org/10.1016/0006-2952\(73\)90196-2](https://doi.org/10.1016/0006-2952(73)90196-2).
- [28] Vrang N, Madsen AN, Tang-Christensen M, Hansen G, Larsen PJ. PYY(3-36) reduces food intake and body weight and improves insulin sensitivity in rodent models of diet-induced obesity. *Am J Physiol Regul Integr Comp Physiol* 2006;291:R367–75. <https://doi.org/10.1152/ajpregu.00726.2005>.
- [29] Hansen HH, Perens J, Roostalu U, Skytte JL, Salinas CG, Barkholt P, et al. Whole-brain activation signatures of weight-lowering drugs. *Mol Metabol* 2021;47:101171. <https://doi.org/10.1016/j.molmet.2021.101171>.
- [30] Arrubla J, Schoelch C, Plum-Moerschel L, Kaptiza C, Lamers D, Thamer C, et al. Phase I study of glucagon-like peptide-1/glucagon receptor dual agonist BI 456906 in obesity (poster 231). *Obesity* 2021;29:139–40. <https://doi.org/10.1002/oby.23329>.
- [31] Gehlert DR, Beavers LS, Johnson D, Gackenhaimer SL, Schober DA, Gadski RA. Expression cloning of a human brain neuropeptide Y Y2 receptor. *Mol Pharmacol* 1996;49:224–8.
- [32] Hu H, Ransdell AS, Qu H, Durbin JD, Valenzuela FA, Hernandez-Buquer S, et al. Probing the binding mechanism of acylated peptides to human serum albumin. *ACS Chem Biol* 2023;18:1158–67. <https://doi.org/10.1021/acscchembio.3c00018>.
- [33] Thomas L, Martel E, Rist W, Uphues I, Hamprecht D, Neubauer H, et al. The dual GCGR/GLP-1R agonist survodutide: biomarkers and pharmacological profiling for clinical candidate selection. *Diabetes Obes Metabol* 2024;26:2368–78. <https://doi.org/10.1111/dom.15551>.
- [34] Milliken BT, Eifers C, Chepurny OG, Chichura KS, Sweet IR, Borner T, et al. Design and evaluation of peptide dual-agonists of GLP-1 and NPY2 receptors for glucoregulation and weight loss with mitigated nausea and emesis. *J Med Chem* 2021;64:1127–38. <https://doi.org/10.1021/acs.jmedchem.0c01783>.
- [35] Acosta A, Hurtado MD, Gorbatyuk O, La Sala M, Duncan D, Aslanidi G, et al. Salivary PYY: a putative bypass to satiety. *PLoS One* 2011;6:e26137. <https://doi.org/10.1371/journal.pone.0026137>.
- [36] Hurtado MD, Acosta A, Riveros PP, Baum BJ, Ukhanov K, Brown AR, et al. Distribution of Y-receptors in murine lingual epithelia. *PLoS One* 2012;7:e46358. <https://doi.org/10.1371/journal.pone.0046358>.
- [37] Kowalczyk R, Harris PWR, Williams GM, Yang SH, Brimble MA. Peptide lipidation - a synthetic strategy to afford peptide based therapeutics. *Adv Exp Med Biol* 2017;1030:185–227. [https://doi.org/10.1007/978-3-319-66095-0\\_9](https://doi.org/10.1007/978-3-319-66095-0_9).
- [38] Bech EM, Kaiser A, Bellmann-Sickert K, Nielsen SS, Sørensen KK, Elster L, et al. Half-life extending modifications of peptide YY(3-36) direct receptor-mediated internalization. *Mol Pharm* 2019;16:3665–77. <https://doi.org/10.1021/acs.molpharmaceut.9b00554>.
- [39] Knudsen LB, Lau J. The discovery and development of liraglutide and semaglutide. *Front Endocrinol* 2019;10:155. <https://doi.org/10.3389/fendo.2019.00155>.
- [40] Østergaard S, Paulsson JF, Kofoed J, Zosel F, Olsen J, Jeppesen CB, et al. The effect of fatty diacid acylation of human PYY(3-36) on Y(2) receptor potency and half-life in minipigs. *Sci Rep* 2021;11:21179. <https://doi.org/10.1038/s41598-021-00654-3>.
- [41] Lucey M, Pickford P, Bitsi S, Minnion J, Ungewiss J, Schoeneberg K, et al. Disconnect between signalling potency and *in vivo* efficacy of pharmacokinetically optimised biased glucagon-like peptide-1 receptor agonists. *Mol Metabol* 2020;37:100991. <https://doi.org/10.1016/j.molmet.2020.100991>.
- [42] Simonsen L, Lau J, Kruse T, Guo T, McGuire J, Jeppesen JF, et al. Preclinical evaluation of a protracted GLP-1/glucagon receptor co-agonist: translational difficulties and pitfalls. *PLoS One* 2022;17:e0264974. <https://doi.org/10.1371/journal.pone.0264974>.
- [43] Moran TH, Smedh U, Kinzig KP, Scott KA, Knipp S, Ladenheim EE. Peptide YY(3-36) inhibits gastric emptying and produces acute reductions in food intake in rhesus monkeys. *Am J Physiol Regul Integr Comp Physiol* 2005;288:R384–8. <https://doi.org/10.1152/ajpregu.00535.2004>.
- [44] Witte AB, Gryback P, Holst JJ, Hilsted L, Hellstrom PM, Jacobsson H, et al. Differential effect of PYY1-36 and PYY3-36 on gastric emptying in man. *Regul Pept* 2009;158:57–62. <https://doi.org/10.1016/j.regpep.2009.07.013>.
- [45] Rangwala SM, D'Aquino K, Zhang YM, Bader L, Edwards W, Zheng S, et al. A long-acting PYY(3-36) analog mediates robust anorectic efficacy with minimal emesis in nonhuman primates. *Cell Metab* 2019;29:837–843 e835. <https://doi.org/10.1016/j.cmet.2019.01.017>.
- [46] Beetz N, Kalsch B, Forst T, Schmid B, Schultz A, Hennige AM. A randomized phase I study of BI 1820237, a novel neuropeptide Y receptor type 2 agonist, alone or in combination with low-dose liraglutide in otherwise healthy men with overweight or obesity. *Diabetes Obes Metabol* 2025;27:71–80. <https://doi.org/10.1111/dom.15984>.
- [47] Ortiz AA, Milardo LF, DeCarr LB, Buckholz TM, Mays MR, Claus TH, et al. A novel long-acting selective neuropeptide Y2 receptor polyethylene glycol-conjugated peptide agonist reduces food intake and body weight and improves glucose metabolism in rodents. *J Pharmacol Exp Therapeut* 2007;323:692–700. <https://doi.org/10.1124/jpet.107.125211>.
- [48] Tschoep M, Castaneda TR, Joost HG, Thone-Reineke C, Ortman S, Klaus S, et al. Physiology: does gut hormone PYY3-36 decrease food intake in rodents? *Nature* 2004;430. <https://doi.org/10.1038/nature02665>. 1 p following 165; discussion 2 p following 165.
- [49] Ziffert I, Kaiser A, Babilon S, Morl K, Beck-Sickinger AG. Unusually persistent G $\alpha_i$ -signaling of the neuropeptide Y(2) receptor depletes cellular G $\beta\gamma$  pools and leads to a G $\beta\gamma$ -refractory state. *Cell Commun Signal* 2020;18:49. <https://doi.org/10.1186/s12964-020-00537-6>.
- [50] Shi YC, Ip CK, Reed F, Sarruf DA, Wulff BS, Herzog H. Y5 receptor signalling counteracts the anorectic effects of PYY3-36 in diet-induced obese mice. *J Neuroendocrinol* 2017;29. <https://doi.org/10.1111/jne.12483>.
- [51] Acuna-Goycolea C, van den Pol AN. Peptide YY(3-36) inhibits both anorexigenic proopiomelanocortin and orexigenic neuropeptide Y neurons: implications for hypothalamic regulation of energy homeostasis. *J Neurosci* 2005;25:10510–9. <https://doi.org/10.1523/JNEUROSCI.2552-05.2005>.

- [52] Huston NJ, Brenner LA, Taylor ZC, Ritter RC. NPY2 receptor activation in the dorsal vagal complex increases food intake and attenuates CCK-induced satiation in male rats. *Am J Physiol Regul Integr Comp Physiol* 2019;316:R406–16. <https://doi.org/10.1152/ajpregu.00011.2019>.
- [53] Fetissov SO, Kopp J, Hokfelt T. Distribution of NPY receptors in the hypothalamus. *Neuropeptides* 2004;38:175–88. <https://doi.org/10.1016/j.npep.2004.05.009>.
- [54] Jais A, Bruning JC. Arcuate nucleus-dependent regulation of metabolism-pathways to obesity and diabetes mellitus. *Endocr Rev* 2022;43:314–28. <https://doi.org/10.1210/endrev/bnab025>.
- [55] Gabery S, Salinas CG, Paulsen SJ, Ahnfelt-Rønne J, Alanentalo T, Baquero AF, et al. Semaglutide lowers body weight in rodents via distributed neural pathways. *JCI Insight* 2020;5. <https://doi.org/10.1172/jci.insight.133429>.
- [56] Skovbjerg G, Roostalu U, Hansen HH, Lutz TA, Le Foll C, Salinas CG, et al. Whole-brain mapping of amylin-induced neuronal activity in receptor activity-modifying protein 1/3 knockout mice. *Eur J Neurosci* 2021. <https://doi.org/10.1111/ejn.15254>.
- [57] Chepurny OG, Bonaccorso RL, Leech CA, Wollert T, Langford GM, Schwede F, et al. Chimeric peptide EP45 as a dual agonist at GLP-1 and NPY2R receptors. *Sci Rep* 2018;8:3749. <https://doi.org/10.1038/s41598-018-22106-1>.
- [58] Zimmermann T, Thomas L, Baader-Pagler T, Haebel P, Simon E, Reindl W, et al. BI 456906: discovery and preclinical pharmacology of a novel GCGR/GLP-1R dual agonist with robust anti-obesity efficacy. *Mol Metabol* 2022;66:101633. <https://doi.org/10.1016/j.molmet.2022.101633>.